Numerical analysis of the volume of cavitation cloud in a cavitation tunnel using multiphase computational fluid dynamics simulations

Robert Jasionowski[1]✉, Waldemar Kostrzewa[2]

[1] https://orcid.org/0000-0002-2943-3593
[2] https://orcid.org/0000-0002-9614-3086

Maritime University of Szczecin, Department of Machine Construction and Materials
2-4 Willowa St., 71-650 Szczecin, Poland
e-mail: [1]r.jasionowski@pm.szczecin.pl, [2]w.kostrzewa@pm.szczecin.pl
✉ corresponding author

Abstract
This work is devoted to a computational investigation of the position and volume of the cavitation cloud in a cavitation tunnel. The position of the cavitation cloud and its volume in the cavitation tunnel, determined by numerical analysis with respect to the inlet velocity, allows for the determination of the lower or higher intensity of cavitation erosion within the tunnel of the sample material. A numerical analysis is carried out on a model of a typical cavitation tunnel used to investigate the resistance of structural materials to cavitation erosion. The tunnel under study consists of barricade (upper) and counter-barricade (lower) systems. The numerical analysis is carried out with the following five different values of the velocity in the tunnel inlet: 6 m/s, 9 m/s, 12 m/s, 15 m/s, and 18 m/s in the commercial CFD software – Ansys Fluent 2019 R3. The Schnerr and Sauer cavitation model and shear stress transport (SST) viscous model k-omega are used. The paper analyzes the distribution of velocity, pressure, and volume of the cavitation cloud. On the basis of the performed numerical analyses, the optimal velocity at the inlet to the tunnel of 15 m/s is determined, for which the volume of the cavitation cloud is the largest and the phenomenon of cavitation is the most intense. The determination of the position and maximum volume of the cavitation cloud relative to the inlet velocity to the tunnel will, in future, allow us to shorten the resistance tests for cavitation erosion of different materials under real fluid flow conditions.

Introduction

Multiphase flow occurs in many different natural phenomena as well as in many technological processes. A multiphase flow is an arrangement of at least two different substances or different states of concentration of the same substance mixed together in any ratio and exhibiting individual properties as a whole. For multiphase flows, we deal with homogeneous and inhomogeneous flows. Understanding multiphase flow is very difficult due to various physical phenomena. One of the natural phenomena in which multiphase flow occurs is the phenomenon of cavitation (Biesheuvel & Van Wijngaarden, 1984; de Crecy, 1986; Riznic & Ishii, 1989; Kolev, 2007; 2015).

Cavitation is the process of formation, growth, and implosion of bubbles containing steam, gas, or steam-gas mixture due to cyclic pressure changes in the flowing liquid (Plesset, 1949; Plesset

& Chapman, 1971; Plesset & Prosperetti, 1977; Gibson & Blacke, 1982; Brennen, 1995; Franc & Michel, 2004). The implosion of cavitation is an effect of pressure change from an area of low value to a region of elevated pressure, causing condensation of steam that fills the cavitation bubble. The implosion phenomenon occurs at very high velocities (exceeding 100 m/s) and, in such cases, the growth and decay time of the cavitation bubble is in the order of milliseconds. According to previous research (Plesset & Chapman, 1971), the dynamics of the formation and sealing of the bubble are dependent on the physicochemical properties of the liquid, the distance between the wall, and the interaction of the bubbles. The neighborhood of the wall creates a bubble in the imploding microstream, which can reach a velocity of 300–500 m/s (Fedotkin & Yochno, 2001).

Microstreams formed during the implosion of cavitational bubbles transmit wall pressure pulses in the order of 1–4 GPa. Multiple repetitive cavitation implosion causes vibration of walls, and then elastic and plastic deformation of the surface. According to earlier work (Hickling & Plesset, 1963), only microstreams of bubbles that are located away from the wall at a distance no greater than the radius of the largest bubble have the pressure that causes the destruction of the material. Cavitation occurs in commonly used hydraulic machines such as pumps, turbines, and propellers. The phenomenon of cavitation causes a decrease in the efficiency of hydraulic machinery, increasing noise and vibration (Grist, 1998; Franc & Michel, 2004; Szala & Łukasik, 2016).

Computational fluid dynamics (CFD) is a useful tool for analyzing multiphase flows, including cavitation phenomena. For computer simulations using CFD, the phenomenon of cavitation bubble formation and disappearance is based on the Rayleigh-Plesset equation (Brennen, 1995), i.e.:

$$R\frac{d^2R}{dt^2} + \frac{3}{2}\left(\frac{dR}{dt}\right)^2 = \frac{p_{sat} - p}{\rho_l} - \frac{2\sigma}{\rho_l R} - 4\frac{\mu_l}{\rho_l R}\frac{dR}{dt}$$

(1)

where R represents the bubble radius (in units of m), p_{sat} signifies saturated vapor pressure (Pa), p is the local fluid pressure (Pa), ρ_l is the liquid density (kg/m³), σ is the surface tension (N/m), and μ_l is the dynamic viscosity of liquid (Pas).

The Rayleigh-Plesset equation (1), describing the formation and disappearance of cavitation bubbles, omits viscosity phenomena and surface tensions.

Therefore, current CFD models used for cavitation phenomena are based on the application of a barotropic equation of state to the density of the mixture as a function of local pressure. The basic equation for multiphase cavitation modeling consists of using the standard viscous flow equations governing the transport of mixture (mixture model) or phases (Eulerian multiphase) and a conventional turbulence model (k-ε model). In cavitation, the liquid-vapor mass transfer (evaporation and condensation) is governed by the vapor transport equation:

$$\frac{\partial}{\partial t}(\alpha\rho_v) + \nabla(\alpha\rho_v \vec{V}_v) = R_e - R_c$$

(2)

where α denotes the vapor volume fraction, ρ_v is the vapor density (kg/m³), $\vec{V}_v$ is the vapor phase velocity, R_e is the liquid-vapor mass transfer (evaporation), and R_c is the liquid-vapor mass transfer (condensation).

Among the most common cavitation models in computational fluid dynamics (CFD) liquids are the:

1. Schnerr and Sauer Model – a cavitation model that assumes the existence of two phases: liquid and its vapor. In addition to the basic balance equations mass, momentum, and energy, the steam-phase mass balance equation is solved (Schnerr & Sauer, 2001):

$$p \le p_{sat}, \quad R_e = \frac{\rho_l\rho_v}{\rho}\alpha_v(1-\alpha_v)\frac{3}{R}\sqrt{\frac{2}{3}\frac{p_{sat} - p}{\rho_l}}$$

$$p > p_{sat}, \quad R_c = \frac{\rho_l - \rho_v}{\rho}\alpha_v(1-\alpha_v)\frac{3}{R}\sqrt{\frac{2}{3}\frac{p - p_{sat}}{\rho_l}}$$

(3)

where signifies p is the local fluid pressure (Pa), p_{sat} is the saturated vapor pressure (Pa), R_e is the liquid-vapor mass transfer (evaporation), R_c is the liquid-vapor mass transfer (condensation), ρ_l is the liquid density (kg/m³), ρ_v is the vapor density (kg/m³), ρ is the mixture density (kg/m³), α_v is the vapor volume fraction, and R is the bubble radius (m).

2. Zwart-Gerber-Belamri Model. In this cavitation model, the total interphase mass transfer rate per unit volume is calculated using bubble density numbers and a single bubble mass rate. Zwart-Gerber-Belamri proposed to replace α with α_{nuc}. Then, the final form of this cavitation model is as follows (Zwart, Gerber & Belamri, 2004):

$p \leq p_{\text{sat}}$

$$R_e = C_e \frac{3\alpha_{\text{nuc}}(1-\alpha_v)\rho_v}{R} \sqrt{\frac{2}{3} \frac{p_{\text{sat}} - p}{\rho_l}}, \quad C_e = 50$$

$p > p_{\text{sat}}$

$$R_c = C_c \frac{3\alpha_v \rho_v}{R} \sqrt{\frac{2}{3} \frac{p - p_{\text{sat}}}{\rho_l}}, \quad C_c = 0.01$$

(4)

where p denotes the local fluid pressure (Pa), p_{sat} is the saturated vapor pressure (Pa), C_e is the evaporation coefficient, C_c is the condensation coefficient, R_e is the liquid-vapor mass transfer (evaporation), R_c is the liquid-vapor mass transfer (condensation), ρ_l is the liquid density (kg/m³), ρ_v is the vapor density (kg/m³), ρ is the mixture density (kg/m³), α_v is the vapor volume fraction, and R is the bubble radius (m).

3. Singhal Model – a homogeneous model of cavitation assuming the existence of three phases: liquid, its vapor, and dissolved gas. In addition to the basic mass, momentum, and energy balance equations, the steam-phase mass balance equation is solved (Singhal et al., 2002; Kozubková, Rautová & Bojko, 2012):

$$\frac{\partial}{\partial t}(\alpha\rho_v) + \nabla(\alpha\rho_v \vec{V}_v) = \nabla(\Gamma \nabla \alpha) + R_e - R_c \quad (5)$$

$p \leq p_{\text{sat}}$

$$R_e = C_e \frac{V_{ch}}{\sigma} \rho_l \rho_v \sqrt{\frac{2}{3} \frac{p_{\text{sat}} - p}{\rho_l}} (1-f), \quad C_e = 0.02$$

$p > p_{\text{sat}}$

$$R_c = C_c \frac{V_{ch}}{\sigma} \sqrt{\frac{2}{3} \frac{p - p_{\text{sat}}}{\rho_l}} f, \quad C_c = 0.01$$

(6)

where α represents vapor volume fraction, ρ_v denotes the vapor density (kg/m³), $\vec{V}_v$ signifies vapor phase velocity, Γ is the diffusion coefficient, R_e is the liquid-vapor mass transfer (evaporation), R_c is the liquid-vapor mass transfer (condensation), p is the local fluid pressure (Pa), p_{sat} is the saturated vapor pressure (Pa), C_e is the evaporation coefficient, C_c is the condensation coefficient, V_{ch} is the characteristic velocity, which is an approach from local turbulent geometry $V_{ch} = \sqrt{k}$, σ is the surface tension (N/m), ρ_l is the liquid density (kg/m³), ρ is the mixture density (kg/m³), and f is the vapor mass fraction.

The vapor volume fraction α is deduced from f as:

$$\alpha = f \frac{\rho}{\rho_v} \quad (7)$$

Where α signifies the vapor volume fraction, f is the vapor mass fraction, ρ is the mixture density (kg/m³), and ρ_v is the vapor density (kg/m³).

The mathematical models presented above also have their limitations. None of the cavitation models can be used with the volume of fluid method (VOF) model because the surface tracking schemes for the VOF model are incompatible with the interpenetrating continua assumption of the cavitation models. Additionally, the Singhal model requires the primary phase to be liquid and the secondary phase to be steam and cannot be used with the Euler multiphase model, while Zwart-Gerber-Belamri and Schnerr and Sauer models do not take the effect of noncondensable gases into account by default.

Despite the above limitations, the presented cavitation models are used in the design of hydraulic machines to minimize the phenomenon of cavitation, as well as cavitation erosion studies (Dular & Coutier-Delgosha, 2009; Patella, Archer & Flageul, 2012; Brusiani, Falfari & Bianchi, 2015; Kumar & Bhingole, 2015; Parsi et al., 2017). The CFD are also ideal for the design of cavitation research stations. The latter are often characterized by a different intensity of cavitational destruction, which results in the same test material being tested at different stations and may have a completely different destruction mechanism (Jasionowski, Polkowski & Zasada, 2016, Jasionowski, Zasada & Polkowski, 2016).

This paper presents the results of the analysis of liquid flowing through a cavitation tunnel at different flow velocities, forming a cavitation cloud of different volumes. The main objective of the numerical studies is to optimize the flow parameters in terms of the formation of the largest volume of cavitation. Determining the optimal flow conditions, and thus finding the largest volume of cavitation near the sample, reduces the time of the experimental studies, as well as provides information on the optimal distribution of measuring and control equipment.

Numerical model

Physical model

In the present work, a cavitation tunnel (Figure 1) as part of a cavitation resistance measurement device is subjected to the analysis. The cavitation

tunnel shown in Figure 1 is a typical test device for the resistance of materials to cavitation erosion, consisting of barricade (upper) and counter-barricade (lower) systems.
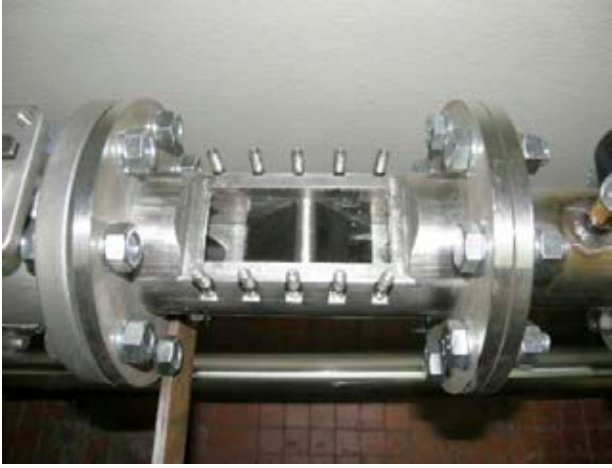

Figure 1. Cavitation tunnel (Jasionowski & Kostrzewa, 2018)

A PML2 80/200 type pump driven by a 15 kW engine and an LG iG5A inverter pushes water through the tunnel. The application of the LG iG5A inverter allows for setting a freely chosen rotational speed of the rotor, thus controlling the flow rate.

The geometric model of cavitation tunnel

The geometric model of the cavitation tunnel was designed in AutoDesk Inventor software using a dimensional accuracy of 0.1 mm. The geometric model of a cavitation tunnel is made of six own-designed components (i.e., a body, a cover, barricades systems, two flanges, and 53 components from pre-existed libraries (Figure 2)).
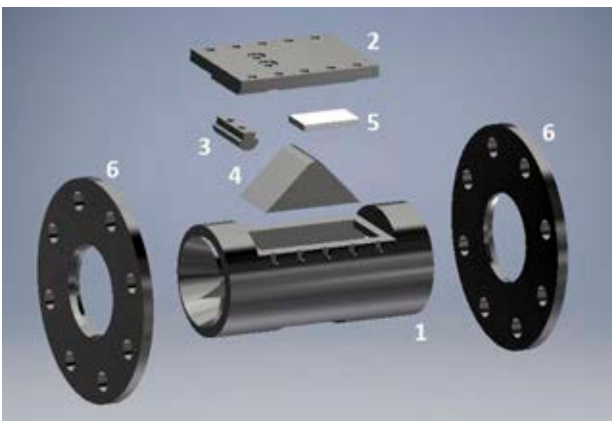

Figure 2. Geometric model with components: 1 – body, 2 – cover, 3 – upper barricade, 4 – lower barricade, 5 – sample, and 6 – flange (Jasionowski & Kostrzewa, 2018)

Meshing and boundary conditions

In this paper, the numerical simulations for the cavitation tunnel were executed using the commercial CFD software – Ansys Fluent 2019 R3. The numerical simulations of the water-vapor-phase flows were carried out in a cavitation tunnel to study the volume of the cavitation cloud. The Schnerr and Sauer cavitation model was chosen for a CFD simulation. The chosen multiphase model (the Schnerr and Sauer Model) will best simulate the cavitation two-phase flow (water-vapor) in the cavitation tunnel. The meshing for the cavitation tunnel was generated using an ANSYS Fluent 2019 R3. A polyhedral mesh was used for numerical analysis of the cavitation tunnel. The volume mesh model consisted of 6,625,695 nodes and 1,668,183 cells (Figure 3). In the middle and outlet parts of the cavitation tunnel, local sizing was applied. Meshing was finalized after a proper checking of the mesh independence of the simulation results.
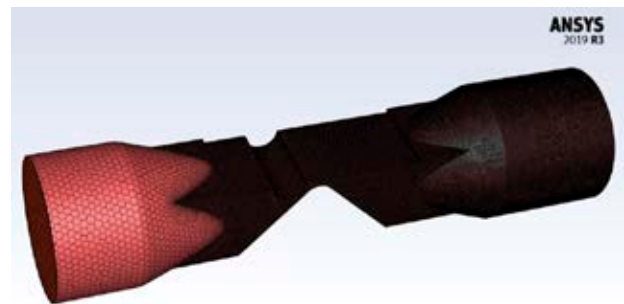

Figure 3. Volume mesh model

The numerical analysis was carried out by using a liquid temperature of 25 °C and the following five different values of the velocity in the tunnel inlet were employed: 6 m/s, 9 m/s, 12 m/s, 15 m/s, and 18 m/s. The following physical parameters were used for water: a density of 0.9882 g/cm^3 and a viscosity of 1003 μPa·s. For vapor: a density of 0.5542 g/cm^3 and a viscosity of 13.4 μPa·s.

Cavitation model and solver setup

Selection of the cavitation model is very important for a multiphase flow analysis. Therefore, in this study, the Schnerr and Sauer cavitation model and the shear stress transport (SST) viscous model k-omega were used. The coupled algorithm was employed for the pressure-velocity coupling with the PRESTO! discretization scheme applied for the pressure (Ansys, 2021). The quadratic
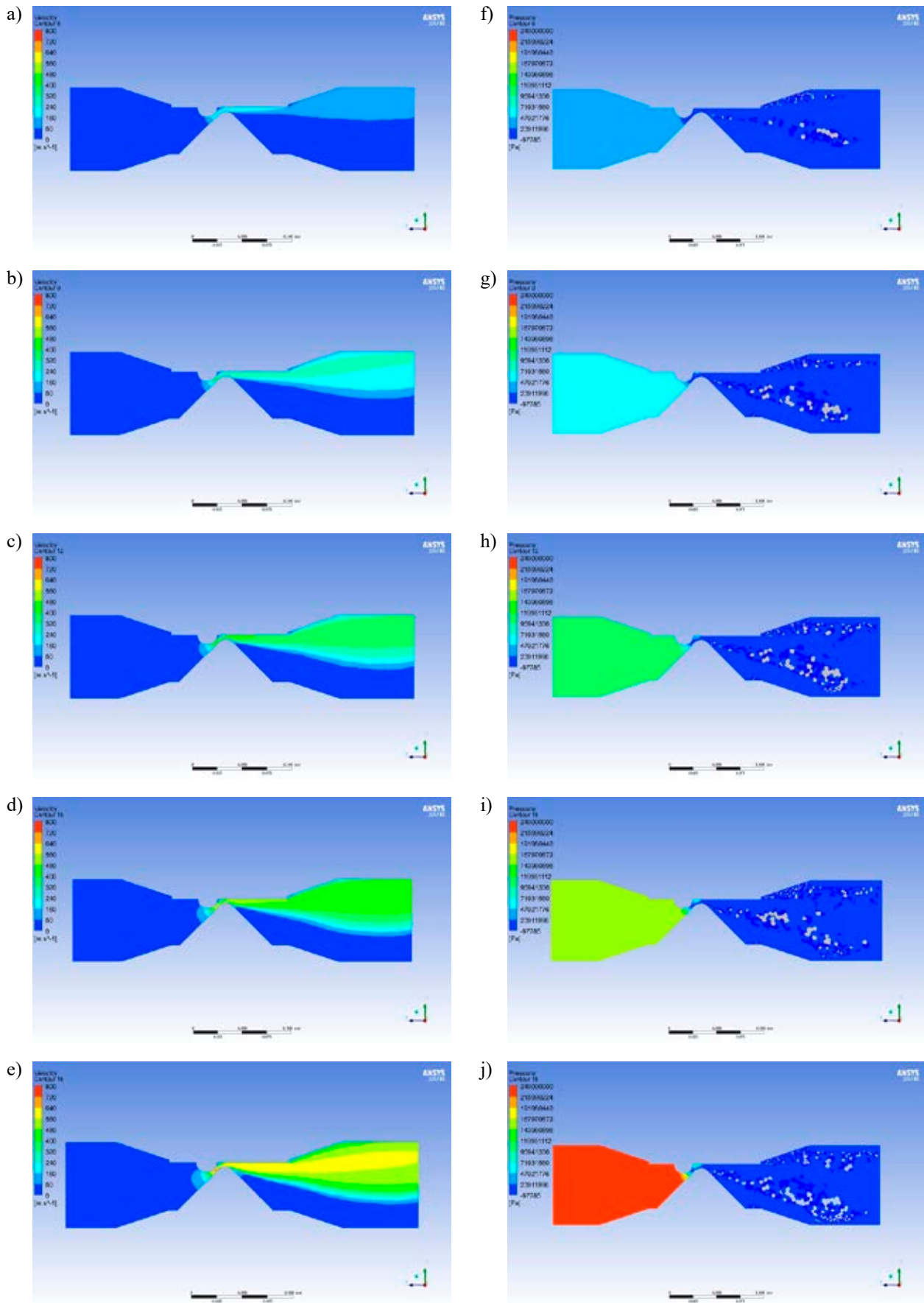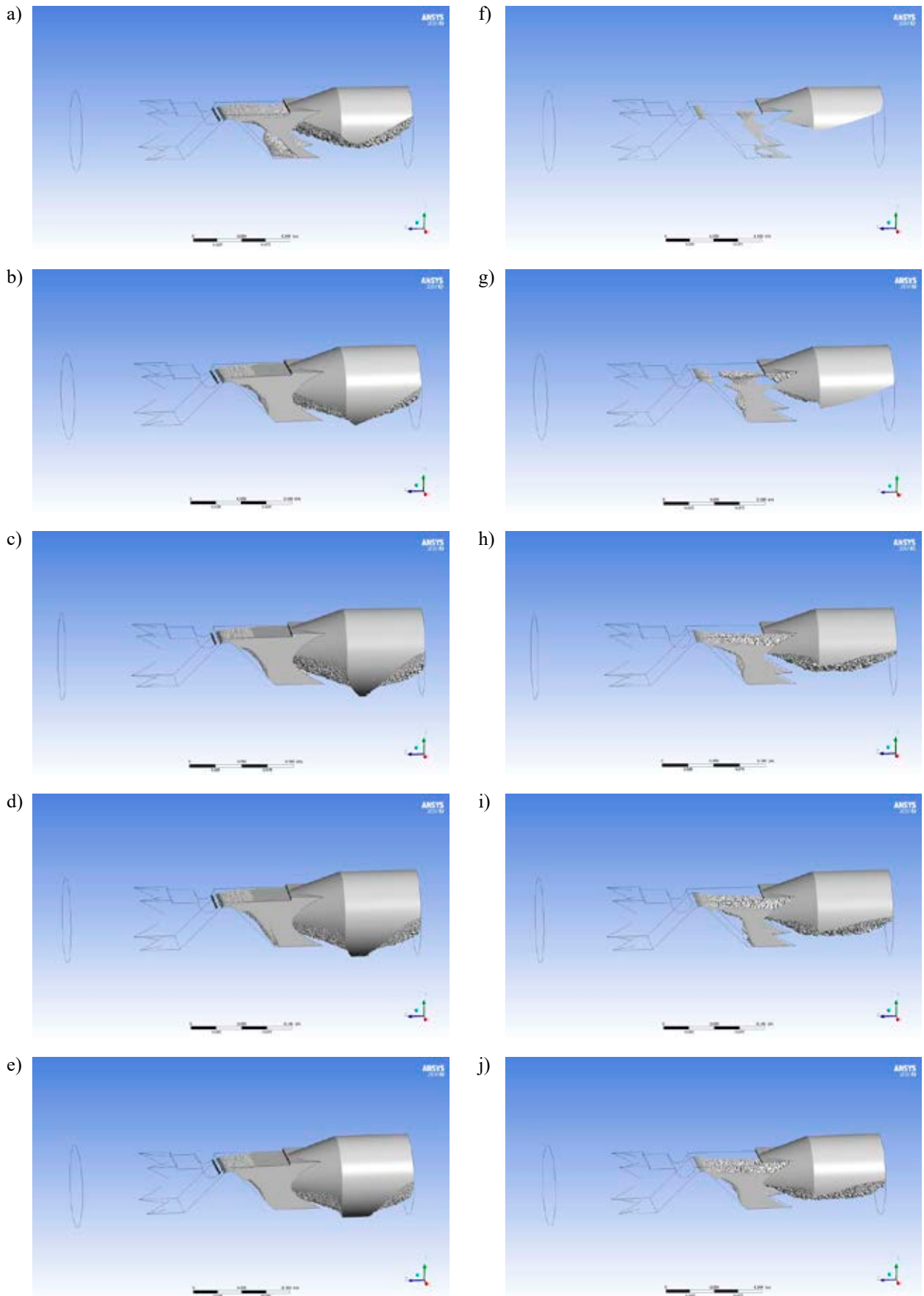
Figure 4. Velocity distribution in the vertical plane: a) 6 m/s, b) 9 m/s, c) 12 m/s, d) 15 m/s, and e) 18 m/s. Pressure distribution in the vertical plane: f) 6 m/s, g) 9 m/s, h) 12 m/s, i) 15 m/s, and j) 18 m/s

Figure 5. Volume vapor fraction between 0.1 and 0.99% vapor: a) 6 m/s, b) 9 m/s, c) 12 m/s, d) 15 m/s, and e) 18 m/s. Volume vapor fraction between 0.9 and 0.99% vapor: f) 6 m/s, g) 9 m/s, h) 12 m/s, i) 15 m/s, and j) 18 m/s

upwind interpolation for the convection kinematics (First Order Upwind) scheme was used to discretize the transport equation for the volume fraction of vapor. The details of the models and schemes used in the multiphase cavitating system are given in Table 1. The numerical analysis of a cavitation cloud in the flow tunnel for each tested velocity had 500 iterations.

Table 1. List of different models and schemes used for modeling the multiphase flow

Name	Model / Scheme Name
Multiphase Flow	Mixture
Cavitation Model	Schnerr-Sauer
Viscous Model	k-omega
k-omega Model	Shear Stress Transport (SST)
Pressure–Velocity Coupling	Coupled Scheme
Spatial Discretization–Gradient	Least Squares Cell Based
Spatial Discretization–Pressure	PRESTO!
Spatial Discretization–Momentum	First Order Upwind
Spatial Discretization–Volume Fraction	First Order Upwind
Spatial Discretization–Turbulent Kinetic Energy	First Order Upwind
Spatial Discretization–Specific Dissination Rate	First Order Upwind

Results

Velocity distribution in the cavitation tunnel

Figure 4 shows the velocity distribution in a cavitation tunnel in the vertical plane (Figure 4 (a)–(e)). The studies have shown that with an increase in the entrance velocity to the tunnel, the velocity between the barricades increases and reaches a maximum velocity in the cavitation tunnel of 843 m/s for the last variant of the test (i.e., 18 m/s). The numerical analyses showed an increase of about 35 times for the velocity between the barricades for all tested flow velocities compared to the inlet velocity to the cavitation tunnel.

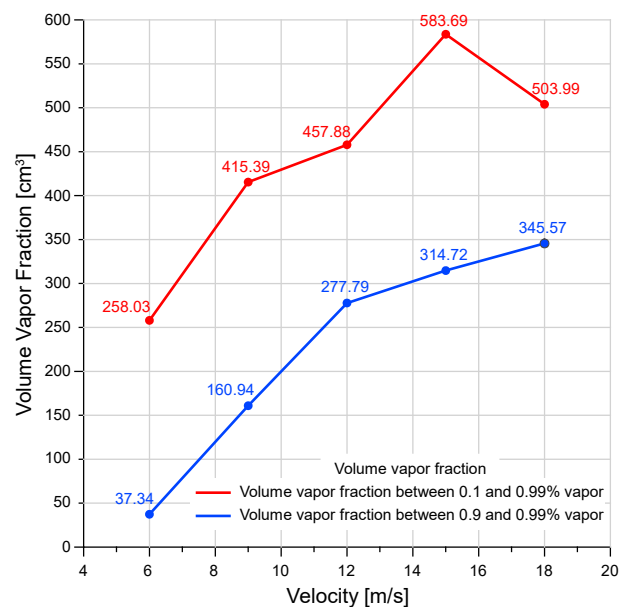### Pressure distribution in the cavitation tunnel

Pressure distribution in the cavitation tunnel is shown in the vertical planes (Figure 4 (f)–(j)). The analyses of the pressure distribution carried out in the vertical plane allow for the establishment of the phenomenon of cavitation, in which an area of the cavitation tunnel is under pressure. The volume

that is under pressure in the cavitation tunnel for each flow rate begins behind the top of the lower barricade for each velocity analyzed. Numerical simulations have shown that a higher velocity at the inlet to the cavitation tunnel causes pressure to rise through the upper barricade. The highest pressure of more than 240 MPa was found for a velocity of 18 m/s at the inlet to the cavitation tunnel.

Volume vapor fraction in the cavitation tunnel

The volume vapor fraction in the cavitation tunnel is shown in Figure 5. The volume vapor fraction is a cavitation cloud, an area of highly developed cavitation resulting from the geometry of the cavitation tunnel, velocity, and physical properties of the liquid. A cavitation cloud is an area filled with a vapor-gas mixture or cavitation bubbles filled with gas.

Figures 5 (a)–(e) show a cavitation cloud containing 0.1 to 0.99% vapor. The volume of this cavitation cloud is the total area in which the phenomenon of cavitation occurs. Figures 5 (f)–(k) display a cavitation cloud, where the occurrence of cavitation is very intense and the vapor content ranges from 0.9 to 0.99%. The results of the volume vapor fraction in the cavitation tunnel are summarized in the diagram of Figure 6 for all velocities.

Figure 6. Results of the volume vapor fraction in the cavitation tunnel for all velocities

Conclusions

Cavitation is a phenomenon in which the phase change from liquid to vapor occurs because the fluid

pressure drops below its vapor pressure. The main cause of vapor generation in cavitation is the pressure drop due to the velocity. The cavitation tunnels are laboratory stands characterized by a similarity of the cavitation course and its varied intensity. In order to understand the formation of the cavitation phenomenon and the appearance and growth of the cavitation cloud, it is worth using numerical CFD simulations, which have proven their worth in the design of hydraulic machinery and equipment.

Numerical CFD simulations for the liquid multiphase flows with five different flow rates (within the range of 6 to 18 m/s) through the cavitation tunnel were carried out in this work. The conducted numerical calculations allowed for determining the distribution of the velocity, pressure, and volume of the cavitation cloud. The following conclusions may be drawn from the obtained results:

- the highest value volume vapor fraction between 0.1 and 0.99% vapor is for a velocity of 15 m/s;
- the highest value volume vapor fraction between 0.9 and 0.99% vapor is for a velocity of 18 m/s;
- the smallest difference between the volume of the cavitation clouds is for the velocities of 12 and 18 m/s;
- when the volume of the cavitation cloud (for the volume vapor fraction between 0.9 and 0.99% vapor) above the velocity of 15 m/s decreases, it can be assumed that the intensity of the cavitation phenomenon is even greater;
- the highest intensity for the cavitation phenomenon (i.e., for a volume vapor fraction between 0.9 and 0.99% vapor) is for speeds ranging from 12 to 18 m/s. The volume of the volume vapor fraction between 0.9 and 0.99% vapor compared to the total volume (a volume vapor fraction between 0.1 and 0.99% vapor) of the cavitation cloud is about 60%;
- the most optimal velocity that creates the cavitation cloud with the highest volume and the most intense cavitation phenomenon, according to the conducted research, is about 15 m/s.

Acknowledgments

References

1. Ansys (2021) *Ansys Fluent User's Guide Release 2021 R2.* Ansys Inc., Canonsburg, USA.

2. Biesheuvel, A. & Van Wijngaarden, L. (1984) Two-phase flow equations for a dilute dispersion of gas bubbles in liquid. *Journal of Fluid Mechanics* 148, pp. 301–318, doi: 10.1017/S0022112084002366.

3. Brennen, C.E. (1995) *Cavitation and bubble dynamics.* Oxford, New York: Oxford University Press.

4. Brusiani, F., Falfari, S. & Bianchi, G.M. (2015) Definition of a CFD multiphase simulation strategy to allow a first evaluation of the cavitation erosion risk inside high-pressure injector. *Energy Procedia* 81, pp. 755–764, doi 10.1016/j.egypro.2015.12.081.

5. de Crecy, F. (1986) Modeling of stratified two-phase flow in pipes, pumps and other devices. *International Journal of Multiphase Flow* 12(3), pp. 307–323, doi: 10.1016/0301-9322(86)90010-8.

6. Dular, M. & Coutier-Delgosha, O. (2009) Numerical modelling of cavitation erosion. *International Journal for Numerical Methods in Fluids* 61(12), pp. 1388–1410, doi: 10.1002/fld.2003.

7. Fedotkin, I. & Yochno, O. (2001) *Some problems of development of cavitation technologies for industry applications.* CAV2001.

8. Franc, J.-P. & Michel, J.-M. (2004) *Fundamentals of Cavitation.* Springer Dordrecht, doi: 10.1007/1-4020-2233-6.

9. Gibson, D.C. & Blacke, J.R. (1982) The growth and collapse of bubbles near deformable surface. *Applied Scientific Research* 38, pp. 215–224.

10. Grist, E. (1998) *Cavitation And The Centrifugal Pump: A Guide For Pump Users.* CRC Press.

11. Hickling, R. & Plesset, M.S. (1963) *The collapse of a spherical cavity in a compressible liquid.* California Institute of Technology.

12. Jasionowski, R. & Kostrzewa, W. (2018) Optimization of geometry of cavitational tunnel using CFD method. In: Awrejcewicz, J. (eds) *Dynamical Systems in Applications. DSTA 2017. Springer Proceedings in Mathematics & Statistics* 249, Springer, Cham, pp. 181–192, doi: 10.1007/978-3-319-96601-4_17.

13. Jasionowski, R., Polkowski, W. & Zasada, D. (2016) Destruction mechanism of ZnAl4 as cast alloy subjected to cavitational erosion using different laboratory stands. *Archives of Foundry Engineering,* 16(1), pp. 19–24, doi: 10.1515/afe-2015-0096.

14. Jasionowski, R., Zasada, D. & Polkowski, W. (2016) The evaluation of the cavitational damage in MgAl2Si alloy using various laboratory stands. *Solid State Phenomena* 252, pp. 61–70, doi: 10.4028/www.scientific.net/SSP.252.61.

15. Kolev, N.I. (2007) *Multiphase Flow Dynamics 2. Thermal and Mechanical Interactions.* 3rd Edition. Berlin, Heidelberg: Springer-Verlag.

16. Kolev, N.I. (2015) *Multiphase Flow Dynamics 1. Fundamentals.* Springer, Cham, doi: 10.1007/978-3-319-15296-7.

17. Kozubková, M., Rautová, J. & Bojko, M. (2012) Mathematical model of cavitation and modelling of fluid flow in cone. *Procedia Engineering* 39, pp. 9–18, doi: 10.1016/j.proeng.2012.07.002.

18. Kumar, D. & Bhingole, P.P. (2015) CFD based analysis of combined effect of cavitation and silt erosion on Kaplan turbine. *Materials Today: Proceedings* 2(4–5), pp. 2314–2322, doi: 10.1016/j.matpr.2015.07.276.

19. Parsi, M., Kara, M., Agrawal, M., Kesana, N., Jatale, A., Sharma, P. & Shirazi, S. (2017) CFD simulation of sand particle erosion under multiphase flow conditions. *Wear* 376–377, Part B, pp. 1176–1184, doi: 10.1016/j.wear.2016.12.021.

20. Patella, R.F., Archer, A. & Flageul, C. (2012) Numerical and experimental investigations on cavitation erosion. *IOP Conference Series: Earth and Environmental Science* 15, 022013, doi: 10.1088/1755-1315/15/2/022013.

21. Plesset, M.S. (1949) The dynamics of cavitation bubbles. *ASME Journal Applied Mechanics* 16(3), pp. 277–282, doi: 10.1115/1.4009975.

22. Plesset, M.S. & Chapman, R.B. (1971) Collapse of an initially spherical vapor cavity in the neighborhood of solid boundary. *Journal of Fluid Mechanics* 47(2), pp. 283–290, doi: 10.1017/S0022112071001058.

23. Plesset, M.S. & Prosperetti, A. (1977) Bubble dynamics and cavitation. *Annual Review of Fluid Mechanics* 9, pp. 145–185, doi: 10.1146/annurev.fl.09.010177.001045.

24. Riznic, J.R. & Ishii, M. (1989) Bubble number density and vapor generation in flushing flow. *International Journal of Heat and Mass Transfer* 32(10), pp. 1821–1833, doi:10.1016/0017-9310(89)90154-3.

25. Schnerr, G.H. & Sauer, J. (2001) *Physical and Numerical Modeling of Unsteady Cavitation Dynamics*. ICMF-2001. 4th International Conference on Multiphase Flow, New Orleans, USA, May 27 – June 1, 2001.

26. Singhal, A.K., Athavale, M.M., Li, H.Y. & Jiang, Y. (2002) Mathematical Basis and Validation of the Full Cavitation Model. *Journal of Fluids Engineering* 124(3), pp. 617–624, doi: 10.1115/1.1486223.

27. Szala, M. & Łukasik, D. (2016) Cavitation wear of pump impellers. *Journal of Technology and Exploitation in Mechanical Engineering* 2(1), pp. 40–44, doi: 10.35784/jteme.337.

28. Zwart, J., Gerber, A.G. & Belamri, T. (2004) *Two-Phase Flow Model for Predicting Cavitation Dynamics*. ICMF 2004. International Conference on Multiphase Flow, Yokohama, Japan, May 30 – June 3, 2004, Paper No. 152.